NANO LETTERS

2007
Vol. 7, No. 5
1424−1427

# Direct Observation of Nanomechanical Properties of Chromatin in Living Cells

**Anthony H. B. de Vries,[†,‡] Bea E Krenn,[§] Roel van Driel,[§] Vinod Subramaniam,[†] and Johannes S. Kanger*[,†]**

*Biophysical Engineering, Faculty of Science and Technology, Institute for Biomedical Technology (BMTI), University of Twente, P.O. Box 217, 7500 AE Enschede, The Netherlands, and Swammerdam Institute for Life Sciences, BioCentrum Amsterdam, University of Amsterdam, Kruislaan 318, 1098 SM Amsterdam, The Netherlands*

*Received March 14, 2007; Revised Manuscript Received April 10, 2007*

## ABSTRACT

**Precise manipulation of nanometer-sized magnetic particles using magnetic tweezers has yielded insights into the rheology of the cell cytoplasm. We present first results using this approach to study the nanomechanics of the cell nucleus. Using a custom-designed micro-magnetic-tweezers instrument, we can achieve sufficiently high magnetic forces enabling the application and measurement of controlled distortion of the internal nuclear structure on the nanometer scale. We precisely measure the elasticity and viscosity inside the nucleus of living HeLa cells. The high value of the Young's modulus ($Y = 2.5 \times 10^2$ Pa) measured relative to the cytoplasm is explained by a large-scale model for in vivo chromatin structure using a polymer network model.**

Proper functioning of biological processes in living cells strongly depends on specific spatial compartmentalization of molecules in addition to chemical and molecular specificity.[1] Detailed knowledge about spatial organization in cells is therefore crucial to the understanding of the molecular processes that govern cell function. A striking example is the regulation of gene expression. Gene expression is modulated at two levels, that of the individual genes, employing transcription factors, promoters, and enhancers, and at the epigenetic level, involving changes in chromatin structure.[2] Several studies have shown that chromatin is organized in numerous compact domains separated by DNA-poor interchromatin regions.[3] Transcription takes place predominantly at the periphery of these domains.[4] The growing awareness of the importance of the physical properties of chromatin in understanding genome function has inspired a variety of studies aimed at characterizing the mechanical properties of chromatin.[5] Thus far, such studies have been limited to reconstituted single chromatin fibers and to isolated chromosomes only.[6] Here we describe and apply a novel method combining microfabrication technology, magnetic tweezers, and nanomanipulation that allows the study of nanomechanical properties of chromatin inside the nucleus of living cells.

Magnetic tweezers (MT) have been used to study a variety of biological and mechanical properties of cells. To this end small magnetic beads are introduced into the cell and the response of the beads to an external magnetic force is measured. The local mechanical properties of intracellular structures such as the cytoskeleton can be derived from these observations. So far this method has been applied exclusively to the cytoplasm of the cell. Applications in the cell nucleus are limited by the requirement of relatively small beads and the corresponding difficulty of exerting commensurately high forces on these beads. We demonstrate in this report that the stiffness of the interior of the nucleus is much larger than that of the cytoplasm; that is, a much higher force is required to evoke a measurable displacement of the magnetic bead. The results set strict limits on polymer models that are used to describe in vivo chromatin organization. We propose a large-scale model for in vivo chromatin structure that correctly predicts the observed nanomechanical behavior of in vivo chromatin

Recently we developed a multipole high force micromachined MT setup that is capable of exerting forces up to a 100-fold larger than those compared to previously developed multipole MT setups.[7] The multipole character of the MT allows for multidirectional manipulation of the beads whereas the high force (>100 pN) allows for the manipulation of small (~500 nm radius) magnetic beads on a nanometer scale inside the nucleus.

A schematic drawing of the magnetic tweezers setup is shown in Figure 1a. A macroscopic magnetic yoke accom-

* Corresponding author. E-mail: j.s.kanger@utwente.nl.
[†] University of Twente.
[‡] Present address: Max Planck Institute for Biophysical Chemistry, Department of Molecular Biology, Am Fassberg 11, 37077 Göttingen, Germany.
[§] University of Amsterdam.

10.1021/nl070603+ CCC: $37.00 © 2007 American Chemical Society
**Published on Web 04/24/2007**

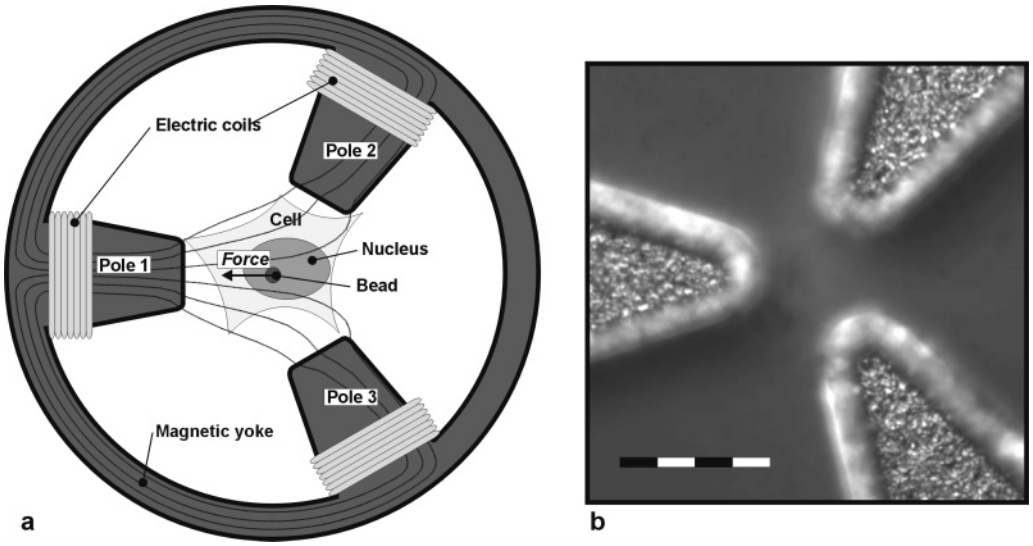


**Figure 1.** (a) Scheme of the micromechanical experiments. Magnetic poles (6 $\mu$m wide, 20 $\mu$m separation) generate a force on a paramagnetic bead positioned in the nucleus of a HeLa cell. Electric coils allow the control of amplitude and direction of the force. Magnetic yoke and electric coils are not to scale. (b) Light microscopy image showing a detail of the cobalt poles geometry (scale bar is 20 $\mu$m).

modates three electric coils that are used to generate the magnetic flux that is guided to the three magnetic poles. The coils can be individually addressed to control the amplitude and direction of the magnetic flux gradient, which is proportional to the exerted force, at the position of the cell. The extremities of the three pole tips were positioned on a circle with a 20 $\mu$m radius leaving a working area of 20 $\times$ 20 $\mu$m$^2$, enabling the positioning of a single cell. A three-pole system yields a uniform force field within the central 10 $\times$ 10 $\mu$m$^2$ and allows full two-dimensional manipulation of the bead within the nucleus of the cell.[7] Due to their small dimensions, the poles are fabricated using cleanroom technology as described elsewhere.[8] In brief, cobalt is electroplated onto glass substrates into a predefined pattern defined by a photoresist layer to yield cobalt poles of well-defined shape and thickness ($\sim$8 $\mu$m) (Figure 1b). Cobalt was chosen for its relatively high saturation magnetization of 1.8 T and its resistance to aqueous environments.

We followed the trajectory of a magnetic bead inside the cell nucleus in response to well-defined magnetic forces exerted in specified directions. The apparatus was used to exert directional forces toward a given pole on submicrometer-sized magnetic beads that were microinjected into the nucleus of a HeLa cell. HeLa cells expressing green fluorescent protein (GFP)-tagged histone H2B, uniformly labeling all the chromatin, were deposited on a glass cover slip and left for 2 h to attach and spread. A single MyOne magnetic bead (Dynal Biotech, Oslo, Norway) (0.5 $\mu$m radius) was aspirated onto a micropipet TIP04TW1F, 0.4 $\mu$m i.d. (World Precision Instruments Inc., Sarasota, FL) connected to a FemtoJet microinjector (Eppendorf AG, Hamburg, Germany). The bead was then positioned inside the nucleus of the cell using a micromanipulator. Subsequently the air pressure inside the pipet was increased to release the bead. Microinjection and nanomanipulation were performed under continuous observation using a white light microscope. No morphological changes (e.g., swelling or blebs formation) of the cell and the nucleus were observed, ensuring that the cells remained vital during the experiments. The direction of the magnetic force on the bead was changed stepwise in a clockwise manner around the poles. Thus the force is first directed toward pole 1 (see Figure 1a), then sequentially toward poles 2 and 3, and finally back toward pole 1. This cycle is continuously repeated using a square alternating current of 33% duty cycle at 0.1 Hz. The square current waveform is used to ensure a stepwise change in direction of the magnetic force and facilitates the data analysis. Experiments were performed at two different amplitudes of the exerted force ($1.1 \times 10^2$ and $6.5 \times 10^1$ pN). Bead displacements were determined by video analysis. The response curves were obtained by averaging nine individual traces for a single cell. In total four cells were measured out of which three cells showed measurable bead displacements.

The measured bead positions (Figure 2) describe a triangular path (a single triangular path is shown) that remained constant over the time period of the experiment ($\sim$2 min). Upon change in the direction of the force, the bead initially shows a fast displacement in the direction of the applied force to a point where it seems to settle until the direction of the force is again changed. This behavior results in the three "clouds" of data points as visible in Figure 2 and is indicative of predominantly elastic rather than viscous behavior. The observed spread in bead positions within a single "cloud" is solely determined by experimental errors mainly originating from the video analysis algorithm, a finding confirmed by measurements on beads that were fixed on glass slides. The amplitude of the movement was proportional to the strength of the exerted force, indicating that the response of the bead is governed by (visco-)elastic behavior. The measured response curves were curve fitted using an analytical model describing the bead motions in a rheological environment called a Voigt−Maxwell body (Figure 3, inset), which consists of a series system of a

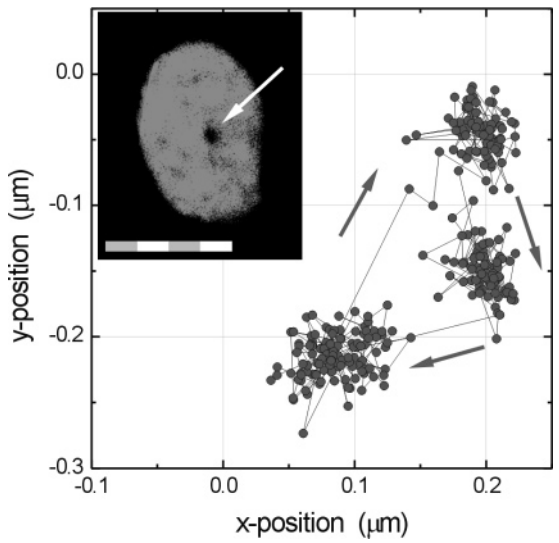


**Figure 2.** Measured trajectory of a magnetic bead inside the nucleus of a living HeLa cell induced by a magnetic force of 110 pN alternating clockwise between three different directions indicated by the arrows. A single triangular path is shown. The inset represents a confocal section through the nucleus of the HeLa cell showing the distribution of GFP-tagged histone H2B. The nucleus contains a single microinjected bead indicated by the arrow. Scale bar is 10 $\mu$m.

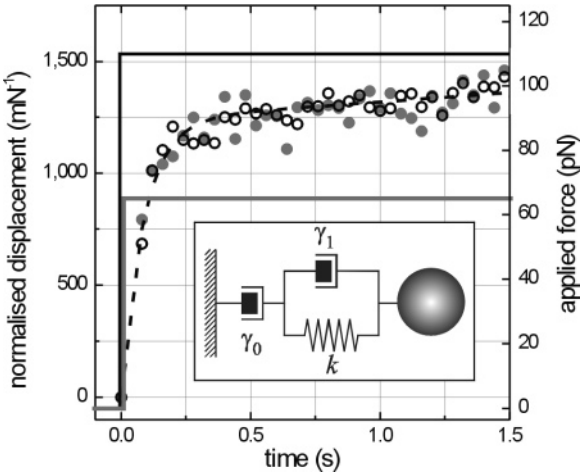


**Figure 3.** Measured response function, normalized by force (left axis), of a bead in the nucleus after application of 65 pN (solid circles) and 110 pN (open circles) force steps (solid, right axis). The dashed line is a curve fit using a viscoelastic model, characterized by damping coefficients $\gamma_0$ and $\gamma_1$ and by a spring constant $k$, as shown in the inset.

viscoelastic body (a dashpot characterized by damping coefficient $\gamma_1$ in parallel with a spring with spring constant $k$) with a dashpot characterized by damping coefficient $\gamma_0$.[9] Using these parameters the viscoelastic properties of the cell nucleus can be extracted. The viscosity $\eta$ is related by Stokes' law: $\eta = \gamma/6\pi r$, where $r$ is the bead radius. The elasticity of the medium is characterized by the Young's modulus $Y$, expressed as $Y = 3\mu$, where $\mu$ is the shear modulus[10] and relates to the measured spring constant as $\mu = k/6\pi r$.[11] From the curve fit (Figure 3) we find: $k = 8.0 \times 10^{-4}$ Pa·m; $\gamma_0 = 1.2 \times 10^{-2}$ Pa·s·m; $\gamma_1 = 7.0 \times 10^{-5}$ Pa·s·m, yielding $\eta_0 = 1.2 \times 10^3$ Pa·s; $\eta_1 = 7.0$ Pa·s, $\mu = 8.5 \times 10^1$ Pa, and $Y = 2.5 \times 10^2$ Pa, where the parameters $k$, $\gamma_0$, $\gamma_1$, $\mu$, $\eta_0$, and $\eta_1$ are as defined as above. Fitting errors were ~10%. The data showed some anisotropic viscoelastic behavior. However the values of the Young's modulus derived from displacements along the different legs of the triangular path varied only ~50%, which does not seriously affect the quantitative modeling of the data. Measurements on the different cells were all within the 50% error margin.

Using a simple polymer model for the chromatin fiber in the nucleus, the data obtained yield parameters concurrent with the current view on interphase chromatin. The general view of chromatin structure in interphase nuclei is one in which the 10 nm nucleosomal chain is folded into a helical structure called the 30 nm fiber which in turn is organized in a so far unknown higher order structure.[12] We treat the 30 nm fiber as a flexible polymer. First we model this polymer as a confined Gaussian chain, which has been used previously to successfully explain the dependence of the average geometric distance between two marked chromosome locations on their genomic separation.[13] In this model chromatin is described as a chain of $N$ segments with length $b$, where $b$ is the Kuhn segment length, which can be approximated by the persistence length $L_p$ of the polymer. For the 30 nm fiber $L_p \approx 30$ nm.[6] In the nucleus each chromosome occupies an exclusive territory not intruded by chromatin from other chromosomes.[3] If a territory is described as a box with dimensions of length $L$ and volume $V$, the pressure $P$ exerted by the bead on the surface orthogonal to length $L$ is given by $P = (\pi^2/3)(b^2/L^2)(NkT/V)$.[14] Assuming that a bead displacement $\Delta x$ induces an equal change in $L$, the corresponding spring constant $k$ for small displacements $\Delta x$ is given by $k \approx (PV)/(L\Delta x) = 2.5 \times 10^{-7}$ Pa·m (with $N = 3.6 \times 10^4$; $V = 11$ $\mu$m$^3$; $L = 2.2$ $\mu$m; $\Delta x =$ 150 nm). This value is much lower than the experimentally observed value ($8.0 \times 10^{-4}$ Pa·m). Clearly this model fails to explain the observed mechanical properties of chromatin.

An alternative approach is to model chromatin structure as a cross-linked polymer network. It makes no difference whether the cross-links are between different polymer molecules or between different sites on a single long polymer molecule. Increasing the cross-linker density $n$ results in a stiffer network: $Y = 6nk_BT$ where $k_B = 1.3 \times 10^{-23}$ J/K is Boltzmann's constant and $T$ is the absolute temperature.[15] On average, the distance between cross-links $\xi$ (written as $\xi^3 = 1/n$) can never exceed the length of the fiber between two cross-links, therefore limiting $n$, and depends on the total volume of the nucleus $V$ and the total length $L$ of the fiber: $n \leq (L/2V)^{3/2}$. The distance between cross-links is calculated (using $V = 315$ $\mu$m$^3$; $L = 5.5 \times 10^{-2}$ m) as $\xi = 1.1 \times 10^2$ nm, and the corresponding length of the fiber between two cross-links is calculated to be much (three times) larger than the persistence length of the 30 nm fiber justifying the use of the polymer network model chosen here and the corresponding expression for the Young's modulus. If we assume that the chromatin fiber is evenly distributed and fills the whole volume of the nucleus, we find a maximum value of the Young's modulus, $Y \leq 0.2 \times 10^2$ Pa, which is in better

agreement with the experimental results than the confined Gaussian chain model. Note however that the calculated value is still smaller than the experimentally observed value which may be explained by realizing that chromatin is organized in individual chromosomes that are spatially confined to specific territories, leaving a considerable inter-chromosomal space containing little or no chromatin.[3] This spatial organization can be taken into account by defining a volume fraction $\Theta$ as the part of the nucleus that is taken up by the sum of all chromosome territories, where $\Theta$ ranges from 0 to 1, and $\Theta = 1$ represents the situation in which chromatin occupies the total nuclear volume. Consequently, the value of the Young's modulus $Y$ of these chromosome territories is given by $Y = 6nk_BT$ with $n \leq (L/2\Theta V)^{(3/2)}$. A volume fraction of $\Theta = 0.19$ yields a maximum value of the Young's modulus $Y \leq 2.5 \times 10^2$ Pa corresponding to the experimental results. However, in this case the length of the fiber between two cross-links is also reduced and approaches the value of the persistence length. Therefore the value of $\Theta$ obtained can be regarded as a lower limit. More advanced modeling is required to correctly include the persistence length of the fiber and to include other factors like the stiffness of the cross-links. Although such a model is beyond the scope of this paper, we continue to develop these ideas in ongoing work. The current model suggests $0.19 < \Theta < 1$, a prediction that is in agreement with current understanding of interphase chromatin organization.

No precise measurements have been made of the nuclear fraction $\Theta$. Electron microscope images of thin sections of nuclei suggest that this value does not exceed 0.5 and might be considerably smaller, depending on the cell type.[16] We speculate that the molecular basis of the cross-linking of the chromatin fiber inside the chromosome territory may be related to the putative arrangement of chromatin in loops.[17] Alternatively, cross-links between nucleosomes may occur via chromatin-associated proteins, such as HP1, which binds to histone H3 methylated at lysine 9 and can form homodimers.[18] However, other chromatin proteins may also be involved, such as the methylated DNA binding protein MeCP2.[19]

We have demonstrated a fruitful new methodology that allows the manipulation of submicrometer magnetic beads inside the nucleus of a living cell to measure local mechanical properties of chromatin structure. The results contribute two important facts to the current discussion on the nature of the nuclear architecture. First, we show that interphase chromatin behaves as an elastic medium. Second, the high value of the Young's modulus may be explained by a polymer network model of chromatin that uses the 30 nm fiber structure as the basic element. This model predicts both a high cross-linker density and agrees with an organization of chromatin fibers in compact chromosome territories.

We believe that the method developed in this paper has numerous applications beyond the study of chromatin organization. Another interesting application would be to use this method to measure forces involved in chromosome rearrangements during cell division. An unexplored but fascinating and challenging possibility is to use functionalized magnetic beads to locally introduce chemical modification of chromatin which may even include localized gene delivery.

**Acknowledgment.** We acknowledge helpful discussions with Jan Greve and Carl Figdor. This work was supported by the foundation for Earth and Life Sciences (ALW), which is subsidized by The Netherlands Organization for Scientific Research (NWO).

## References

(1) Tu, B. P.; Kudlicki, A.; Rowicka, M.; McKnight, S. L. *Science* **2005**, *310* (1575), 1152−1158
(2) van Driel, R.; Fransz, P. F.; Verschure, P. J. *J. Cell Sci.* **2003**, *116*, 4067−4075.
(3) Cremer, T.; Cremer, C. *Nat. Rev. Genet.* **2001**, *2*, 292−301.
(4) Verschure, J. P.; van der Kraan, I.; Manders, E. M.; van Driel, R. *J. Cell Biol.* **1999**, *147*, 13−24.
(5) Marko, J. F.; Poirier, M. G. *Biochem. Cell Biol.* **2003**, *81*, 209−220.
(6) Cui, Y.; Bustamante, C. *Proc. Natl. Acad. Sci. U.S.A.* **2000**, *97*, 127−132.
(7) de Vries, A. H. B.; Krenn, B. E.; van Driel, R.; Kanger, J. S. *Biophys. J.* **2005**, *88*, 2137−2144.
(8) de Vries, A. H. B.; Kanger, J. S.; Krenn, B. E.; van Driel, R. *J. Microelectromech. Syst.* **2004**, *13*, 391−395.
(9) Feneberg, W.; Westphal, M.; Sackmann, E. *Eur. Biophys. J.* **2001**, *30*, 284−294.
(10) Landau, L.; Lifchitz, E. *Theory of elasticity*; Pergamon Press: Oxford, U.K., 1959.
(11) Ziemann, F.; Radler, J.; Sackmann, E. *Biophys. J.* **1994**, *66*, 2210−2216.
(12) Adkins, N. L.; Watts, M.; Georgel, P. T. *Biochim. Biophys. Acta* **2004**, *1677*, 12−23.
(13) Houchmandzadeh, B.; Marko, J. F.; Chatenay, D.; Libchaber, A. *J. Cell Biol.* **1997**, *139*, 1−12.
(14) Doi, M.; Edwards, S. F. *The theory of polymer dynamics*; Claredon Press: Oxford, U.K., 1986.
(15) Doi, M. *Introduction to polymer physics*; Clarendon Press: Oxford, U.K., 1986.
(16) Cmarko, D.; Verschure, P. J.; Otte, A. R.; van Driel, R.; Fakan, S. *J. Cell Sci.* **2003**, *116*, 335−343.
(17) Heng, H. H. Q.; Goetze, S.; Ye, C. J.; Stevens, J. B.; Bremer, S. W.; Wykes, S. M.; Bode, J.; Krawetz, S. A. *J. Cell Sci.* **2004**, *117*, 999−1008.
(18) Eissenberg, J. C.; Elgin, S. C. *Curr. Opin. Genet. Dev.* **2000**, *10*, 204−210.
(19) Georgel, P. T.; Horowitz-Scherer, R. A.; Adkins, N.; Woodcock, C. L.; Wade, P. A.; Hansen, J. C. *J. Biol. Chem.* **2003**, *278*, 32181−32188.

NL070603+